

THE EFFECTS OF CaO CATALYSIS ON THE KINETICS OF NO REDUCTION BY BEULAH ZAP CHAR

Feng Guo and William C. Hecker *

Department of Chemical Engineering and Advanced Combustion Engineering Research Center (ACERC), Brigham Young University, 350 CB, Provo, Utah 84604

Keywords: NO/char reaction; Catalysis; Kinetics.

INTRODUCTION

The reduction of NO emissions from combustion processes has become increasingly important in protecting the world's environment. It has been shown that Selective Catalytic Reduction (SCR) with ammonia is an effective commercial technique to remove NO_x from combustion flue gas. However, the implementation of this technique is limited by high investment and operating costs, "ammonia slip", and SO_x poisoning, which motivate the search for alternatives.¹ Carbon (activated carbon or char) is a promising reducing agent for NO_x reduction with many potential advantages, such as low cost, easy availability, high efficiency, simplicity of process, and no secondary pollution.¹⁻⁷ Moreover, the heterogeneous reaction of NO with char is very important for the understanding of the formation of NO_x from coal combustion processes. The reaction may significantly destroy the NO_x formed earlier in coal combustion, which partially contributes to low NO emission from fluidized bed combustion.^{2,3} Therefore, the reaction of NO with char is receiving significant attention in the literature.

Previous investigations on the reaction of NO with char involve the kinetics and mechanism,⁶⁻²³ the effects of char surface area,^{24,25} the effects of feed gas composition,^{10,7,25} and the catalytic effects of metals.^{5,10,22,26-29} The reaction of NO with char has generally been reported to be first order with respect to NO partial pressure,^{7,13-16} but reaction orders between 0.42 and 0.73 have also been reported.³⁰ A sharp shift in the activation energy has been observed in the temperature range of 873-973 K, which suggests a complex reaction mechanism.^{6,7,15-18} Several mechanisms have been proposed.^{5,6,12,16,18,19,31} However, questions concerning N₂ formation, the surface complexes, the nature of active surface sites, and the effects of minerals in char ash are still not well understood. In most previous studies, chars were taken to be pure carbon, thus the effects of the ash in chars and its composition on the kinetics and mechanism of the reduction reactions are not well known. Although the catalytic effects of certain metals or metal oxides on the reactions have been investigated,^{5,10,22,26-29} little is known about their effects on the kinetics of the reaction. Therefore, the objectives of this study are to investigate the kinetics of the reaction of NO with Beulah Zap chars, to study the effects of CaO on the kinetics.

EXPERIMENTAL METHODS

The chars used in this study were prepared from 63 - 74 μm particles of North Dakota Beulah Zap lignite in a methane flat-flame burner (FFB). Parent char (NDL), a portion of NDL washed with HCl to remove mineral matter (NDW), and a portion of NDW reloaded with calcium oxide (NCa) were used. The CaO contents of NDL, NDW, and NCa are 3.5, 1.1, and 2.4%, respectively. All of these chars were made previously in our laboratory, and details of their preparation were reported elsewhere.^{32,33}

The reduction of NO by char was carried out for all chars at 5 - 6 temperatures between 723 and 1073K in a 10 mm ID VYCOR® glass vertical packed bed reactor with a fritted quartz disc of medium porosity as a support. For each run, 0.2 g char mixed with 2 g silicon carbide (inert materials for the reduction of NO) was packed in the reactor, and heated in He to the maximum temperature desired using an electric furnace. NO diluted with He (3130 ppm of NO) was then fed downward through the reactor for about 1 hour, when a pseudo-steady state was reached. Data were subsequently collected at 5 to 6 flow rate settings between 100 and 500 ml/min (NTP) at each of the temperatures studied. For each run, it took about 4 hours to collect all the data, and the burnout of the char was about 10% during that period of time. The inlet gas pressure in the reactor was controlled at 300 kPa (3 atm). The outlet pressure at each condition was also measured to determine the pressure drop across the packed bed.

The compositions of outlet gases were continuously monitored for N₂, CO, CO₂, N₂O, and O₂ by a GC (Perkin-Elmer, 3920B) with TCD and two columns (one packed with Chromosorb 106, the other packed with molecular sieve 5A), and for NO and NO₂ by a Chemiluminescence NO_x analyzer (Thermo Environmental, 42H). The variations in nitrogen and oxygen mass balances were determined between inlet and outlet streams for each run and always fell within ±5%.

RESULTS AND DISCUSSION

Pretests and Corrections. A typical plot of NO conversion vs. time shows that decreases from 100% to its pseudo-steady state value after about 1 hour. This probably results from NO adsorption on the sample and/or very active char surface sites that are quickly consumed. Thereafter, the conversion of NO decreases very slowly because of the loss of char mass. In order to account for the effect of the char mass loss in the calculation of kinetic parameters, a correction was made based on a carbon mass balance using the following stoichiometric reaction:

$$C + (1+y) \text{NO} = (1-y) \text{CO} + y \text{CO}_2 + 1/2(1+y) \text{N}_2 \quad (1)$$

where $y = [\text{CO}_2]/([\text{CO}] + [\text{CO}_2])$, and $[\text{CO}]$ and $[\text{CO}_2]$ are concentrations of CO and CO_2 , respectively. Since $[\text{CO}]$ and $[\text{CO}_2]$ are measurable quantities, the mass loss of char, ML (g), can be calculated

$$\text{ML} = 12 \cdot t \cdot F_{\text{NO}}^0 \cdot X_{\text{NO}} / (1+y) \quad (2)$$

where t is reaction time elapsed (min); X_{NO} is average conversion of NO in this period; F_{NO}^0 is the inlet molar flow rate of NO (mol/min) calculated from the ideal gas law.

Figure 1 shows the variation of char mass (W) with the NO conversion (X_{NO}) in the form of the integrated rate expression, where the char mass has been corrected using Eq. 2, for the beginning and end of run. Since both sets of values fit the same straight line, the effect of the char mass loss on the reaction rate constant has been eliminated.

As mentioned, the inlet reactor pressures was typically 3.0 atm., but the outlet pressures varied with flow rate. In the calculation of concentration used in the kinetic rate expression, an average pressure $P = (P_{\text{in}} + P_{\text{out}})/2$ was used. Figure 2 shows how using this approach gives kinetic data that all fell on the same straight line for runs in which the pressure was varied (P_{in} from 1.5 to 3.0 atm. and P_{out} from 1.2 to 2.8 atm.) and the total flow rate was varied.

The calculation of film mass transfer and pore diffusion resistances for a worst case scenario (the maximum particle diameter, the minimum flow rate, and the maximum reaction rate observed) indicated that film mass transfer (maximum MT resistance = 2.7%) and pore diffusion (minimum effectiveness factor = 0.99) were negligible in this study.

Kinetics. Because a broad range of NO conversion was observed in this study, the reactor was modeled as an integral plug flow reactor. The reaction rate constants and reaction order were obtained by integral analysis of the experimental data. Briefly, the differential form of the plug flow reactor performance equation is

$$dW/F_{\text{NO}}^0 = dX_{\text{NO}} / -r_{\text{NO}} \quad (3)$$

If the reaction is first order in NO (as confirmed later), integrating Eq. (3) produces the integrated rate expression as

$$-\ln(1 - X_{\text{NO}}) = k_1 C_{\text{NO}}^0 W/F_{\text{NO}}^0 \quad (4)$$

where X_{NO} = NO conversion (= (moles NO in - moles NO out) / moles NO in); F_{NO}^0 = inlet molar flow rate of NO (moles/s); W = char weight (g); $-r_{\text{NO}}$ = NO depletion rate (moles NO reacted/s*g_char); C_{NO}^0 = initial NO concentration (moles/L); k_1 = first order rate constant (L/s*g_char).

Thus, if experimental data are plotted as $-\ln(1 - X_{\text{NO}})$ vs. $C_{\text{NO}}^0 W/F_{\text{NO}}^0$ and a straight line is obtained that passes through the origin, then evidence of 1st order kinetics is obtained and the slope of the line equals the value of the rate constant, k_1 .

The experimental data for NDL char plotted as $-\ln(1 - X_{\text{NO}})$ vs. $C_{\text{NO}}^0 W/F_{\text{NO}}^0$ are shown in Figure 3, indicating that the reaction is first order with respect to NO. Attempts to fit the data to other orders were made, but straight lines were not obtained for all temperatures. Table 1 lists values for the reaction rate constants, their lower and upper 95% confidence limits, and statistical analysis parameters for NDL char data obtained at 6 different temperatures. The correlation coefficients, t-test values, and F-test values all show that the experimental data were excellently fit by first order kinetics under the experimental conditions. The standard error was typically less than 5%. Similar results were obtained for the other two chars, NDW and NCa.

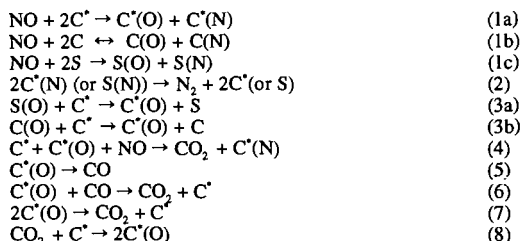
The Effect of CaO. The variations of NO conversion with temperature are shown in Table 2 for three char types at a flow rate of 303 ml/min (NTP). The results for other flow rates are similar. The conversion of NO increases noticeably in the order $\text{NDL} > \text{NCa} > \text{NDW}$. This is in the same order as the CaO content of the three chars, 3.5% > 2.4% > 1.1%. Therefore, the effects of CaO on the reaction of NO with chars appear to be significant.

Figure 4 shows the Arrhenius plots of the rate data for NDL, NDW, and NCa chars. The bars around points in the figure show the variation of the reaction rate constants in 95% confidence level. A sharp shift in the apparent activation energy with temperatures was observed, as also reported in literature.^{6,7,13-18} The temperatures at which the transition takes place are in the range of 823 ~ 973 K, and decrease as the CaO content increases. This shift to higher activation energy with increasing temperature is opposite to the expectation if a reaction is changing from chemical rate control to mass transfer control, and suggests different mechanisms or rate determining steps at high and low temperatures. It is also noted that at low temperatures the apparent activation energies for all three char types are essentially the same (22 ~ 26 kcal/mol); at high temperatures, however, the activation energies vary from 45 to 60 kcal/mol, increasing as the CaO content of the

chars decreases. The variation of the NO reduction reactivity, the apparent activation energy, and the transition temperature with the CaO content are summarized in Table 2.

Discussion. The active surface sites of carbon are generally classified as edge sites and basal sites. At low temperatures, the reactivity of the basal sites can be negligible, compared to that of the edge sites.²¹ In addition to the active sites of carbon, there exist other active sites, including sites on the surface of CaO, K₂O, CuO, and other potential catalysts. These active sites, as chemical or structural impurities, enhance the carbon edge sites; they can also chemisorb NO dissociatively like the carbon active sites. While chemisorbed oxygen migrates to and reacts with the carbon edge sites around, the chemisorption of NO on the inorganic sites continues. Therefore, CaO, K₂O, CuO *etc.* may exhibit catalytic effects on the reaction of NO with char.

The reactivity of NO with char increases significantly with increasing CaO content. Such increase involves two aspects. On one hand, an increase in CaO content provides more defects of coal structure, the reactivity of char then increases; on the other hand, the catalytic effects of CaO also increase due to more active CaO sites. The reaction of NO with char may not proceed as a simple catalytic process. Two routes may exist in parallel, which are the direct reduction of NO on active carbon sites and the catalytic reduction of NO through active CaO sites. When there are enough active CaO available, the catalytic reduction route is predominant. On the other hand, when very few active CaO sites exist, the direct reduction route becomes predominant. Between the two extreme cases, which most actual cases may belong to, the reduction of NO may be controlled by the both routes. Therefore, the two parallel processes should be taken into account in the mechanism of the reaction of NO with char. A possible parallel reaction model may be described as follows:



where C* is the carbon edge sites; C is the basal sites; S is the active sites of catalysts. Reactions 1a, 1b, 1c are parallel processes of the dissociative chemisorption of NO. The desorption of the chemisorbed oxygen involves only the carbon edge sites (C*) represented by Reaction 4, 5, 7, and 8, which are parallel routes. All oxygen atoms adsorbed on the other active sites (C or S) need to migrate to the carbon edge sites before desorption as described by Reaction 3a, 3b. On the bases of the facts of the delay in CO₂ or CO evolution with respect to N₂²⁷⁻²⁹ and the positive effects of O₂ on the reaction of NO with char,³ it is reasonable to assume that the desorption of the chemisorbed oxygen is the rate determining steps. At low temperatures, Reactions 5 and 8 may be slow; therefore, the reaction rate of NO with char may depend on Reactions 4, 6, 7 or a combination of these reactions, and CO₂ is a dominant product of C-containing species; at high temperatures, however, Reactions 5 and 8 become fast, and Reaction 5 will be a major pathway of the desorption of the chemisorbed oxygen, so that Reaction 5 controls the reaction rate of NO with char, and CO becomes a dominant product. With the shift in the rate determining step, the apparent activation energy also changes as shown in Figure 4.

Since the reduction of NO by char is composed of two parallel processes, i.e. the direct reduction of NO on active carbon sites and the catalytic reduction of NO through active CaO sites, it seems that the apparent activation energy for the global reaction of NO with char is a combination of the activation energies of the two parallel processes in some way. When the CaO content (actually the CaO surface area) increases, the proportion of the catalytic reduction may increase. If the activation energy for the catalytic reduction is lower than that for direct reduction (a reasonable assumption), the apparent activation energy will decrease as the CaO content increases as listed in Table 2 for the high temperature data.

CONCLUSION

The kinetics of the reaction of NO with char have been determined for three kinds of chars with different CaO contents. The reaction is first order with respect to NO partial pressure, and has a sharp shift in the activation energy with temperature. The shift temperature decreases as the CaO content in the chars increases. At low temperatures, the activation energies for all three char types are essentially the same (22-26 kcal/mol); at high temperatures, however, the activation energies vary in the range of 45 to 60 kcal/mol, and increase as the CaO content decreases. The migration of the chemisorbed oxygen on basal carbon sites to carbon edge sites at high temperatures may result in a shift in the rate determining step, so that a shift in the activation energy takes place. When the CaO content increases, the activation energy of the migration of the chemisorbed oxygen may decrease; hence, the shift temperature decreases.

Acknowledgments. This work was sponsored by the Advanced Combustion Engineering Research Center at Brigham Young University. Funds for this center are received from the National Science Foundation, the State of Utah, the U. S. Department of Energy, and a number of industrial participants. We also thank Richard F. Cope for char preparation and Troy Ness for technical assistance.

References

- (1) Bosch, H. *Catalysis Today*, 1988, 2, 1.
- (2) Pereira, F. J.; Beer, J. M.; Gibbs, B.; Hedley, A. B. *15th Symposium (International) on Combustion*; The Combustion Institute: Pittsburgh, 1975, p1149.
- (3) Johnson, J. E. *Fuels* 1994, 73, 1398.
- (4) Illan-Gomez, M. J.; Linares-Solano, A.; Salinas-Martinez de Lecea, C. *Energy Fuels* 1993, 7, 146.
- (5) Yamashita, H.; Tomita, A., *Energy Fuels* 1993, 7, 85.
- (6) Teng, H.; Suuberg, E. M.; Calo, J. M. *Energy Fuels* 1992, 6, 398.
- (7) Furusawa, T.; Tsunoda, M.; Tsujimura, M.; Adschiri, T. *Fuel* 1985, 64, 1306.
- (8) Furusawa, T.; Kunii, D.; Osuma, A.; Yamada, N. *Int. Chem. Eng.* 1980, 20, 239.
- (9) Wendt, J. O. L.; Pershing, D. W.; Lee, J. W.; Glass, J. W. *17th Symposium (International) on Combustion*; The Combustion Institute: Pittsburgh, 1979, p77.
- (10) Levy, J.; Chan, L. K.; Sarofim, A. F.; Beer, J. M. *18th Symposium (International) on Combustion*; The Combustion Institute: Pittsburgh, 1981, p111.
- (11) Watts, H. *Trans. Faraday Soc.* 1958, 54, 93.
- (12) Smith, R. N.; Swinehart, J.; Lesnini, D. *J. Phys. Chem.* 1959, 63, 544.
- (13) Richthofen, A. V.; Wendel, E.; Neuschütz, D. *Fresenius' J. Anal. Chem.* 1993, 346, 261
- (14) Edwards, H. W. *AIChE Symp. Ser. No. 126*, 1972, 68, 91.
- (15) Song, Y. H.; Beer, J. M.; Sarofim, A. F. *Combust. Sic. Technol.* 1981, 25, 237.
- (16) Chan, L. K.; Sarofim, A. F.; Beer, J. M. *Combust. Flame* 1983, 52, 37.
- (17) Radovic, L. R.; Walker, Jr., P. L. *Fuel Process Technol.* 1984, 8, 149.
- (18) Suuberg, E. M.; Teng, H.; Calo, J. M. *23rd Symposium (International) on Combustion*; The Combustion Institute: Pittsburgh, 1990; p1199.
- (19) Teng, H.; Suuberg, E. M. *J. Phys. Chem.* 1993, 97, 478.
- (20) Teng, H.; Suuberg, E. M. *Ind. Eng. Chem. Res.* 1993, 32, 416.
- (21) Chu, X.; Schmidt, L. D. *Ind. Eng. Chem. Res.* 1993, 32, 1359.
- (22) Lai, C.-K. S.; Peters, W. A.; Longwell, J. P. *Energy Fuels* 1988, 2, 586.
- (23) Matos, M. A. A.; Pereira, F. J. M. A.; Ventura, J. M. P. *Fuel* 1991, 70, 38.
- (24) Shimizu, T.; Sazawa, Y.; Adschiri, T.; Furusawa, T., *Fuel* 1992, 71, 361.
- (25) Yamashita, H.; Yamada, H.; Tomita, A. *Applied Catalysis*, 1991, 78, L1-L6.
- (26) Furusawa, T.; Koyama, M.; Tsjimura, M. *Fuels* 1985, 64, 413.
- (27) Illan-Gomez, M. J.; Linares-Solano, A.; Radovic, L.; Salinas-Martinez de Lecea, C. *Energy Fuels* 1995, 9, 97.
- (28) Illan-Gomez, M. J.; Linares-Solano, A.; Radovic, L.; Salinas-Martinez de Lecea, C. *Energy Fuels* 1995, 9, 104.
- (29) Illan-Gomez, M. J.; Linares-Solano, A.; Radovic, L.; Salinas-Martinez de Lecea, C. *Energy Fuels* 1995, 9, 112.
- (30) Johnson, J. E.; Dam-Johansen, K. *11th International Conference on Fluidized Bed Combustion*, American Soc. Mech. Eng., New York, 1991, p1389.
- (31) De Soete, G. C. *23rd Symposium (International) on Combustion*; The Combustion Institute: Pittsburgh, 1990; p1257.
- (32) Cope, R. F.; Arrington, C. B.; Hecker, W. C. *Energy fuels* 1994, 8, 1059.
- (33) Cope, R. F. *Dissertation*, Brigham Young University, Provo, Utah, 1995.
- (34) Illan-Gomez, M. J.; Linares-Solano, A.; Radovic, L.; Salinas-Martinez de Lecea, C. 8th International conference on Coal Science, Oviedo, Spain, 1995, p1911.

Table 1 The Reaction Rate Constants of ND L Char and Statistical Analysis

T °C	k ₁ L/sec*g char	k ₁ Low 95%	k ₁ Up 95%	Std Error	Corr Coef	t Test	t-distrib	F Test	F-distrib
					r ²		α=0.01		α=0.01
650	0.0736	0.0562	0.0909	4.03E-03	0.994	18.2	9.925	333	199
625	0.0353	0.0333	0.0373	7.29E-04	0.998	48.5	4.604	2348	26
600	0.0182	0.0161	0.0202	7.40E-04	0.993	24.6	4.604	457	26
600	0.0181	0.0158	0.0205	8.48E-04	0.991	21.4	4.604	604	26
550	0.0070	0.0063	0.0078	2.66E-04	0.994	26.5	4.604	701	26
500	0.0029	0.0026	0.0032	1.10E-04	0.994	26.2	4.604	686	26
470	0.0016	0.0016	0.0017	2.56E-05	0.999	64.1	4.604	4103	26

Table 2 NO Reduction Reactivity, Apparent Activation Energy and Transition Temperature for Three Char types

CaO %	T @50% conv. (Q=303m/m), K	Transition T K	App. Act. Energy (kcal/mol)	
			High Temp	Low Temp
NDL	3.5	875	44.5±5	22.2±3
NCA	2.4	940	53.1±5	26.2±3
NDW	1.1	980	59.5±5	22.7±3

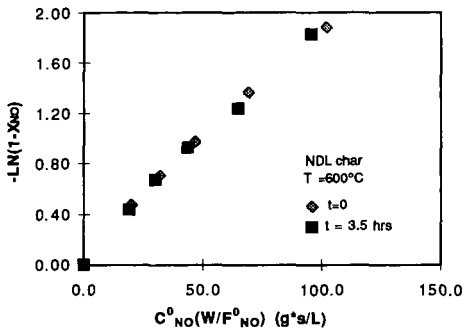


Figure 1 The effect of run time on the integrated rate expression after the char mass loss correction.

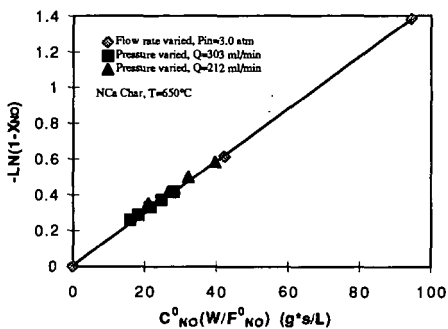


Figure 2 The effect of pressure and flow rate (P_{bed}) on the integrated rate expression, using $P_{bed} = 1/2(P_{in} + P_{out})$.

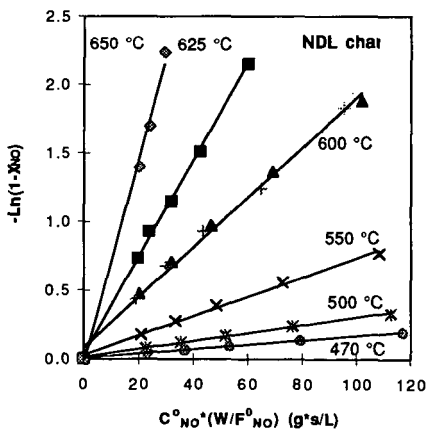


Figure 3 Experimental data for NDl char plotted as $-\ln(1-X_{NO})$ vs. $C_{NO}^0(W/F_{NO}^0)$

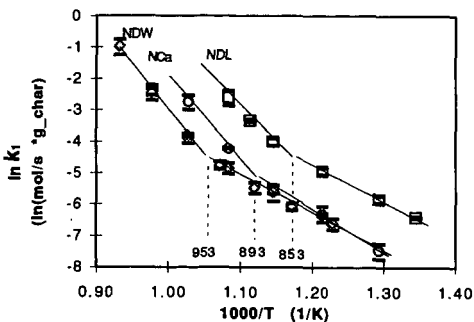


Figure 4 Arrhenius plots of the reaction rate constants for NO reduction with char for three chars.